

A Geometric Model of Retinocortical Mechanisms

Luc Florack*

Abstract

Koenderink’s conjecture that the visual system can be understood as a “geometry engine” is taken as the point of departure for modelling retinocortical mechanisms. A fibre bundle over a Riemannian manifold endowed with a conformal metric, constructed in an axiomatic fashion, is proposed as a geometric model of receptive field assemblies. Phenomenological facts such as the Weber-Fechner law, the retinotopical cortical magnification, and the way in which typical receptive field size scales with eccentricity can be incorporated in a fairly straightforward manner.

1 Introduction

In this article we aim for a theoretical description of retinocortical mechanisms. The stance adopted in the present work is the conjecture raised and explored by Koenderink that the visual system can be understood as a “geometry engine” [13, 15, 24, 25, 26, 30, 18, 27, 16, 17, 19, 31, 20, 32, 21, 22, 29, 33, 23, 34, 28].

Emphasis will be on the potential role geometry could play in understanding retinocortical mechanisms, not on an ultimately realistic description *per se*. That is to say, we take the liberty to make idealisations for the sake of simplicity, but we also provide arguments to justify these. The crucial conjecture is one of *linearity*, the pivotal assumption around which all of geometry evolves, which we justify by proposing an explicit linearisation procedure. In general, we believe that the idealisations made in the theory do not invalidate the approach.

The main advantage of a geometric model is its susceptibility for a systematic refinement. Refinement can be of a retrospective nature (modelling existing empirical facts) as well as, more interestingly, of a propriospective nature (relating potential geometric expertise to actual visual mechanisms).

2 Theory

2.1 Geometric Preliminaries

We introduce a *total space* \mathcal{E} , consisting of *fibres* over a *base manifold* \mathcal{M} , and a *projection map* $\pi : \mathcal{E} \rightarrow \mathcal{M}$. We endow each fibre $\pi^{\text{inv}}(\mathfrak{p}) \subset \mathcal{E}$, $\mathfrak{p} \in \mathcal{M}$, with a vector space

*Utrecht University, Department of Computer Science, Padualaan 14, NL-3584 CH Utrecht, The Netherlands.

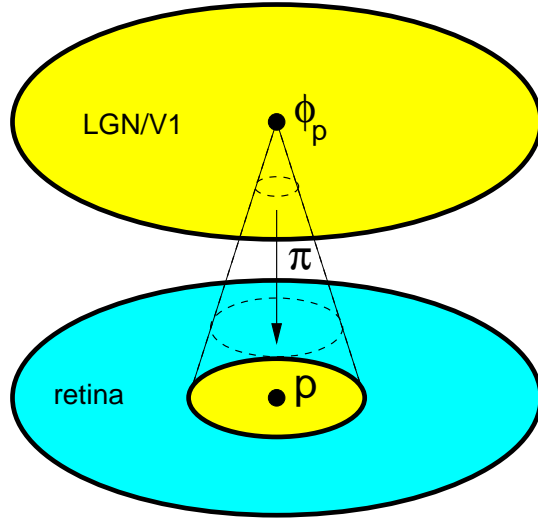


Figure 1: Retina and LGN/V1 viewed as a base manifold, respectively fibre bundle; $p = \pi(\phi_p)$ is a fiducial point on the retina which corresponds retinotopically to the centre point of a receptive field $\phi_p \subset \pi^{\text{inv}}(p)$ in LGN or V1.

structure [40]. Via a suitable coordinatisation we identify $\mathcal{M} \sim \mathbb{R}^n$ with $n = 2$ or 3 depending on whether we consider instantaneous spatial, or spatiotemporal mechanisms (we ignore compactness; this is not essential for subsequent discussions). The totality $(\mathcal{E}, \pi, \mathcal{M})$ endowed with the aforementioned vector space structure constitutes a *fibre bundle*, which we shall henceforth refer to as \mathcal{E} by abuse of notation.

The base manifold is a continuum representing the neural tissue in the retina composed of photoreceptor cells [1, 38]. A fibre is associated with a receptive field assembly at fixed retinal base point $p = \pi(\phi_p)$. This is, ideally, an infinite dimensional linear space, for which we shall take $\mathcal{S}(\mathbb{R}^n)$ in the absence of *a priori* constraints, *i.e.* the class of smooth functions of rapid decay [39]. Retinal irradiance distributions are represented by scalar functions $f \in \mathcal{S}'(\mathbb{R}^n)$. To emphasize the retinal base point of a local receptive field assembly we will write $\mathcal{S}_p(\mathbb{R}^n)$, $\mathcal{S}'_p(\mathbb{R}^n)$, respectively $\mathcal{S}(\mathbb{R}^n) = \cup_p \mathcal{S}_p(\mathbb{R}^n)$ and $\mathcal{S}'(\mathbb{R}^n) = \cup_p \mathcal{S}'_p(\mathbb{R}^n)$. This fibre bundle construct corresponds to the neural substrate of ganglion, simple and complex cells in *retina*, *lateral geniculate nucleus* (LGN) and *striate cortex* (V1). It potentially accounts for retinotopic mappings (via the projection map), hierarchical (intra-fibre) and heterarchical (inter-fibre or connection) structure of receptive field assemblies: Figs. 1 and 2.

The response of a visual neuron in LGN or V1 typically depends on strength and location of the stimulus within a confined region of the retina. The sensitivity as a function of location (and possibly duration) is called the neuron's *receptive field*. If we apply exactly the same stimulus, but monitor the output of a different cell, even if its receptive field has the same base point $p = \pi(\phi_p)$, we generally find a different result. This is why we need a bundle construct; there are many cells “monitoring” any given point in the retina. Likewise, the output of any given photoreceptor in the retina contributes to many receptive fields simultaneously, and therefore it is not sufficient to know only the “raw” retinal signal produced by the photoreceptor units, even though

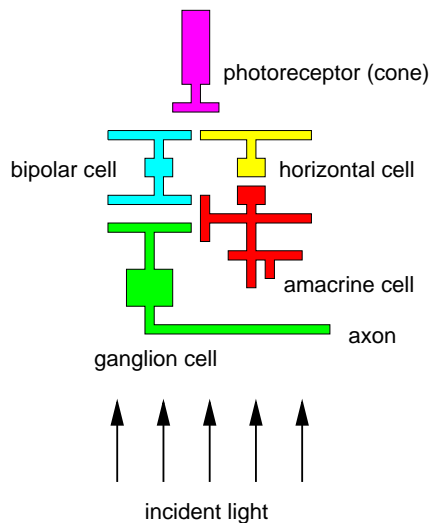


Figure 2: Five classes of retinal neurons (*cf.* Rodieck [38]). Photoreceptors—rods and cones—are stimulated by incident light, and project via bipolar cells onto ganglion cells. Via their axons the visual pathway continues to LGN, V1 and beyond. Horizontal cells antagonize cones, and are laterally interconnected. Cones contribute to the hyperpolarization of the horizontal cell array, which acts in a sign-inverting manner back upon each of the cones, thus antagonizing the effect of their hyperpolarization caused by ambient light. There also exist feedback loops between amacrine and bipolar cells, but feedback pathways always end at ganglion cells, as these are not presynaptic to any other retinal cell. The feedback pathways provided by the amacrine cells almost certainly play significant roles in the regulation of retinal function. In particular, amacrine cells might be responsible for motion preferences displayed by certain ganglion cells.

this contains, strictly speaking, all optical information.

2.2 The Basic Paradigm: Scale Causality

Consider a multiresolution family of functions of the type $u(\mathbf{r}; s)$ with $(\mathbf{r}; s) \in \mathbb{R}^2 \times \mathbb{R}$, in which s parametrises scale. If u is C^1 with respect to s and C^2 with respect to \mathbf{r} , then we can represent the osculating paraboloid to an iso-surface in (\mathbf{r}, s) -space at a spatial extremum—the origin, say—in terms of a so-called Monge patch parametrisation:

$$s = \frac{1}{2} \mathbf{r}^T \mathbf{Q} \mathbf{r} \quad \text{with} \quad \mathbf{Q} = -\frac{1}{u_s} \mathbf{H}. \quad (1)$$

Here, \mathbf{H} is the Hessian matrix of u evaluated at the origin (second order spatial derivatives of u), and u_s is the scale derivative of u . Note that at an extremum the Hessian eigenvalues are either all positive or all negative, so that the corresponding surface is indeed a paraboloid. At the origin its normal coincides with the normal to the original iso-surface, and points towards increasing scale iff (note that the uniform sign of the Hessian eigenvalues equals that of their sum, *i.e.* the Laplacean)

$$u_s \Delta u > 0. \quad (2)$$

The enforcement of this demand is known as the *causality principle* [14]. The simplest *linear* partial differential equation (p.d.e.) that realises this is the isotropic diffusion equation

$$u_s = \Delta u, \quad (3)$$

with $\Delta u = u_{xx} + u_{yy}$ in Cartesian coordinates. This equation will be our point of departure, together with the transformation degrees of freedom that preserve scale causality [8]. Endowed with initial condition $f \in \mathcal{S}'(\mathbb{R}^2)$ —determined by the retinal irradiance distribution—and suitable boundary conditions the full system becomes

$$\begin{cases} u_s & = \Delta u & (x, y; s) \in \Omega_R \times \Sigma \\ \lim_{s \rightarrow 0} u(x, y; s) & = f(x, y) & (x, y) \in \Omega_R \\ u(x, y; s) & = 0 & (x, y; s) \in \partial\Omega_R \times \Sigma, \end{cases} \quad (4)$$

in which $\partial\Omega_R$ is the boundary of an open sphere $\Omega_R : \|\mathbf{r}\|^2 < R^2$ of radius R , $\Sigma = (0, S)$ is an open scale interval. Furthermore, the average of f on Ω_R is assumed to be zero. For simplicity we henceforth assume $\Omega_R = \mathbb{R}^2$ and $\Sigma = \mathbb{R}^+$.

Eq. (4) is a local constraint to be satisfied at any given point $p \in \mathcal{M}$, but can be extended to a p.d.e. defined on all of \mathcal{M} . Not every p.d.e. that is locally equivalent to Eq. (4) has this global form, however.

The solution to Eq. (4) given the initial data $f \in \mathcal{S}'(\mathbb{R}^n)$ is known as the *scale-space representation* of f [8, 14, 35, 41, 12, 43], since it is a representation of f as a function of scale $\sigma = \sqrt{2s}$ (inverse resolution). Of special interest are the self-similarity solutions of Eq. (4), the so-called *Gaussian family* [36], consisting of all derivatives of the zeroth order Gaussian Green's function. These will be our prototypes for modelling receptive field profiles [44, 45, 31]. Let us denote the Gaussian family by $\mathcal{G}(\mathbb{R}^n) = \cup_p \mathcal{G}_p(\mathbb{R}^n)$; note that it is a proper subset of $\mathcal{S}(\mathbb{R}^n)$.

2.3 Extensions of the Basic Equation

One must pay caution when relating a physical quantity (such as the retinal irradiance function u in Eq. (4)) to a psychophysical one, since the parametrisation of the former is essentially arbitrary. The same is *a fortiori* true for all those properties that rely on some preferred parametrisation, notably linearity.

The psychophysically relevant parametrisation is whatever nature has accomplished through evolution. This depends critically on the optical environment of the species of interest. Therefore, consider $u = \gamma(v)$, where γ is a strictly monotonic mapping ($\gamma' > 0$, say). It is easily verified that at the location of an extremum the matrix \mathbf{Q} in Eq. (1) is invariant under this mapping, so that we may conclude that at extrema the convex side of a scale-space iso-surface continues to point in the direction of increasing scale. In other words, monotonic mappings of the type $u = \gamma(v)$ preserve scale causality [10, 9]. Inserting $u = \gamma(v)$ into Eq. (4) we find

$$v_s = \Delta v + \mu \|\nabla v\|^2. \quad (5)$$

in which $\mu = (\ln \gamma)'$. The elliptic operator on the r.h.s. is a “pseudo-linear” Laplacean in the sense that Eq. (5) is just the linear Eq. (4) “in disguise”, which shows that for strictly monotonic mappings—the case of interest here—the linearity assumption entails no loss of generality.

A second extension of the basic equation is obtained if we consider Eq. (4) on a Riemannian manifold. We will denote the retinal manifold endowed with a flat, Euclidean metric by $(\mathcal{M}, \mathbf{h})$. In an arbitrary coordinate frame Eq. (4) then takes the form

$$u_s = \frac{1}{\sqrt{\mathbf{h}}} \nabla_\alpha \left(\sqrt{\mathbf{h}} \mathbf{h}^{\alpha\beta} \nabla_\beta u \right). \quad (6)$$

The elliptic operator on the r.h.s. is the Laplace-Beltrami operator relative to the flat metric \mathbf{h} of $(\mathcal{M}, \mathbf{h})$. The matrix $\mathbf{h}^{\alpha\beta}$ is the inverse of $\mathbf{h}_{\alpha\beta}$ defined through¹ $\mathbf{h} = \mathbf{h}_{\alpha\beta} dx^\alpha \otimes dx^\beta$, and $\mathbf{h} = \det \mathbf{h}_{\alpha\beta}$. In a suitable coordinate system we have $\mathbf{h}_{\alpha\beta} = \delta_{\alpha\beta}$, upon which Eq. (6) reproduces Eq. (4).

Indeed, if $(\mathcal{M}, \mathbf{h})$ is flat, Eq. (6) can be reduced to Eq. (4) by a suitable coordinate reparametrisation [11]. However, we consider the possibility of a retinocortical metric transform, $(\mathcal{M}, \mathbf{h}) \rightarrow (\mathcal{N}, \mathbf{g})$, in which the cortical manifold $(\mathcal{N}, \mathbf{g})$ is not necessarily homogeneous nor even flat. In such a case, Eq. (4) can still be realised locally for each point, but no longer globally.

It should be stressed that the postulate of a retinal or cortical metric does not imply the existence of a *perceptual* metric, in the sense that a human subject should be capable of performing perceptual tasks that imply metrical expertise. The metric introduced here is merely an internal representation of the metric of the spatial environment of the species.

Finally, since the basic equation is an evolution equation, one more option for extension presents itself. We may rescale the scale parameter s in Eq. (4) arbitrarily, and replace it by any admissible reparametrisation.

¹Summation convention applies to repeated indices.

Combining the results of this section we obtain the following p.d.e. model for retinal processing:

$$w_t = \square_{\mathbf{h}, \mu} w \tag{7}$$

$$\stackrel{\text{def}}{=} \frac{1}{\sqrt{\mathbf{h}}} \nabla_{\alpha} \left(\sqrt{\mathbf{h}} \mathbf{h}^{\alpha\beta} \nabla_{\beta} w \right) + \mu \mathbf{h}^{\alpha\beta} \nabla_{\alpha} w \nabla_{\beta} w.$$

The scale parameter has been indicated by t to distinguish it from the one in Eq. (4). The nonlinearity parameter can be related to the so-called Weber-Fechner law, whereas the choice of a suitably chosen, inhomogeneous metric can be related to a foveal mechanism. These are the subjects of the next two sections.

The Gaussian family, *i.e.* the self-similarity solutions of Eq. (4), carries over under the combined transformation to a receptive field family intrinsically connected to Eq. (7).

2.4 Weber-Fechner Law

The Weber-Fechner law is a psychophysical law that applies to various perceptual modalities. It states that the intensity of the percept is a logarithmic function of the intensity of the physical stimulus. Here we consider the relation between apparent brightness v and retinal irradiation u . The Weber-Fechner law is a direct consequence of Eq. (5) if we take μ to be a positive constant. Indeed, in this case one readily finds $\gamma(v)$ to be an exponential function (defined up to a pair of integration constants). If we impose the boundary conditions $\gamma(-\infty) = 0$ and $\gamma(\infty) = \infty$ (so that u is positive definite), and assume that $\gamma(0) = u_0$ for some constant $u_0 > 0$, then we obtain

$$v = \frac{1}{\mu} \ln \frac{u}{u_0}.$$

A least noticeable perceptual difference dv then corresponds to a logarithmic increment $\mu^{-1} du/u$ of photon flux. One could interpret $v_0 = \mu^{-1}$ as a psychophysical unit of dimension for the quantity v . The constant u_0 may be adaptive to ambient light conditions to the extent that the potentially available range of v -values (neural firing patterns in-between threshold and saturation frequencies) is actually realized for a steady stimulus.

Isomorphism between retinal irradiance and perceived brightness is of course merely an idealisation that holds only within certain physical limits and if lateral interactions can be ignored². The Weber-Fechner law, *e.g.*, holds only within an interval of physical photon fluxes of a few orders of magnitude. Threshold and saturation phenomena can, however, be accounted for by the same token, in which case the mapping γ is still one-to-one (for each distinguishable perceptual brightness level there is a unique physical irradiance), but no longer onto (irradiances beyond threshold and saturation cannot be segregated). A way to achieve this is to replace the unbounded mapping γ above by $\gamma_{\chi} = \gamma \circ \chi$ for some suitably chosen psychophysical function χ , such that χ^{inv} is bounded and monotonic, say $\chi^{\text{inv}} : \mathbb{R} \rightarrow (0, 1)$. This amounts to a replacement of the nonlinearity coefficient $\mu \rightarrow \mu_{\chi} = \mu \chi' + \chi''/\chi'$.

²An example of significant lateral interaction arises in the so-called Craik-O'Brien-Cornsweet illusion; adjacent regions of identical luminance separated by a narrow region with a particular transient luminance profile induce distinct brightness percepts.

2.5 Foveation and Cortical Magnification

Retinal processing in mammalian vision is characterised by a foveal mechanism, in which resolution decreases roughly in proportion to eccentricity, *i.e.* the radial distance from an *area centralis* (*e.g.* humans, primates) or the vertical distance from an elongated *visual streak* (*e.g.* rabbit). Foveal mechanisms can be introduced via a metric transform as follows. We consider the rotationally symmetric case only.

Consider a conformal metric transform, or “metric rescaling”, induced by a smooth mapping $\sigma : (\mathcal{M}, \mathbf{h}) \rightarrow (\mathcal{N}, \mathbf{g})$, and define $\mathbf{g}(\mathbf{p}) = \sigma^* \mathbf{h}(\sigma(\mathbf{p}))$:

$$\mathbf{g} = e^{2\zeta} \mathbf{h}, \quad (8)$$

in which $\zeta(r)$, $r = \|\mathbf{r}\|$, is a radially symmetric, smooth scalar function defined everywhere on the retinal manifold except perhaps at the fiducial origin, $\mathbf{r} = 0$, the foveal point. If one departs from an unbiased Euclidean metric \mathbf{h} such a transform induces a spatial bias which depends only on radial distance from the foveal point³. The scalar $\zeta(r)$ can be related to the retinotopic *cortical magnification*; we return to this below.

A special property that holds only for $n = 2$ is that if instead of Eq. (7) we take

$$w_s = \square_{\mathbf{g}, \mu} w, \quad (9)$$

as our basic equation, then using Eq. (8) this can be rewritten as

$$w_s = e^{-2\zeta} \square_{\mathbf{h}, \mu} w. \quad (10)$$

In other words, we can in this case interpret the metric rescaling as a scale rescaling, for if we set

$$t = e^{-2\zeta} s + t_0, \quad (11)$$

for some constant t_0 , then Eq. (10) reduces to Eq. (7). If we set $\tau = \sqrt{2t}$, $\tau_0 = \sqrt{2t_0}$, and reparametrise scale logarithmically, $t = t_0 e^{2\kappa}$, $s = t_0 e^{2\lambda}$, with $\lambda \in \mathbb{R}$ and $\kappa \geq 0$ if $t_0 > 0$ is the smallest scale available, we obtain the following scale-eccentricity law:

$$\kappa(\lambda; \zeta) = \frac{1}{2} \ln (e^{2(\lambda-\zeta)} + 1). \quad (12)$$

Furthermore, the assumption that $(\mathcal{M}, \mathbf{h})$ is flat (has a flat connection, or equivalently, a vanishing Riemann curvature tensor) implies that $(\mathcal{N}, \mathbf{g})$ is flat as well, provided ζ is a harmonic function satisfying the Laplace equation. This follows from the fact that for $n = 2$ the Riemann curvature tensor of $(\mathcal{M}, \mathbf{h})$ is completely determined in terms of the Riemann curvature scalar; if we denote the Riemann curvature scalar for $(\mathcal{M}, \mathbf{h})$ and $(\mathcal{N}, \mathbf{g})$ by $\mathbf{R}_{\mathcal{M}}$, respectively $\mathbf{R}_{\mathcal{N}}$, then the metric rescaling of Eq. (8) yields

$$e^{2\zeta} \mathbf{R}_{\mathcal{N}} = \mathbf{R}_{\mathcal{M}} + 2(n-1)\Delta\zeta + (n-1)(n-2)\|\nabla\zeta\|^2.$$

³In the anisotropic case one often replaces eccentricity by *equivalent eccentricity* to effectively enforce isotropy [38].

The reader is referred to the literature for details [5, 11]. Thus if $\Delta\zeta = 0$ Eq. (8) relates flat metrics defined at different eccentricities $0 \leq r < R$. The solution is

$$\zeta_q(r) = q \ln \frac{r_0}{r}, \quad (13)$$

in which $r_0 > 0$ is some constant radius, which demarcates the transition between the *area centralis* and the periphery, and in which $q \in \mathbb{R}$. The case of interest here is $q = 1$, and we take $\zeta(r) = \zeta_1(r)$ henceforth. If

$$\mathbf{h} = r^2 d\theta \otimes d\theta + dr \otimes dr,$$

then

$$\mathbf{g} = \left(\frac{r_0}{r}\right)^2 (r^2 d\theta \otimes d\theta + dr \otimes dr). \quad (14)$$

If we switch to so-called *log-polar coordinates*⁴, $(\pi, \lambda) \in [0, 2\pi r_0) \times \mathbb{R}$, defined by

$$(\pi, \lambda) = \Xi(\theta, r) : \begin{cases} \pi &= r_0 \theta \\ \lambda &= r_0 \ln \frac{r}{r_0}, \end{cases} \quad (15)$$

then we get $\mathbf{g} = d\pi \otimes d\pi + d\lambda \otimes d\lambda$. This shows that the log-polar transform, Eq. (15), provides a canonical coordinate system in which the metric becomes homogeneous. We can interpret the two-form

$$\Xi^* \epsilon_{\mathcal{M}} = \Xi^* (d\pi \wedge d\lambda) = \left(\frac{r_0}{r}\right)^2 r d\theta \wedge dr = \left(\frac{r_0}{r}\right)^2 \epsilon_{\mathcal{M}},$$

with unit two-form $\epsilon_{\mathcal{M}} \in \Lambda^2(\mathbb{T}\mathcal{M}_p^*)$, as the eccentricity-weighted elementary area element at retinal position $\mathbf{p} : (r, \theta)$. This means that if we disregard resolution limitations the size of equally salient receptive fields should scale in direct proportion to eccentricity r . There is ample evidence for this linear scaling phenomenon from psychophysics [3, 42] as well as from neurophysiology; *e.g.* typical dendritic field diameter of retinal ganglion cells appears to be directly proportional to eccentricity [7, 38]. A better way to see this is to recall Eqs. (9–12) and Eq. (13):

$$\kappa(\lambda; r) = \frac{1}{2} \ln \left(e^{2\lambda} \left(\frac{r}{r_0}\right)^2 + 1 \right), \quad (16)$$

which in fact reveals resolution limitations as well, since it is manifestly positive. For fixed $\lambda \in \mathbb{R}$, Eq. (12) is just an eccentricity dependent scaling of inner scale: Fig. 3. Asymptotically, *i.e.* for large enough eccentricity, Eq. (12) shows receptive field sizes which are directly proportional to eccentricity in the periphery, and approximately constant receptive field sizes near the foveal point. Receptive fields satisfying this scaling behaviour for fixed λ constitute natural spatial assemblies, since they reflect the *a priori*

⁴Strictly speaking polar and log-polar coordinates are not genuine coordinates in the technical sense of being locally diffeomorphic to Cartesian coordinates, due to the singularity at the fovea [40].

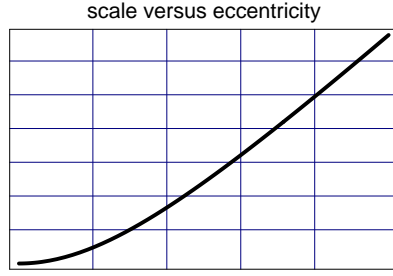


Figure 3: Scale (horizontal axis) *versus* eccentricity (vertical axis). The graph is approximately linear in the periphery, and approximately constant near the foveal point.

spatial bias of the visual system. At each retinal location, however, we may encounter local assemblies of receptive fields parametrised by λ , which also belong together.

With the help of Eq. (16) we can predict the retinotopic cortical magnification m . If we consider a typical receptive field size at eccentricity r by fixing $\lambda = 0$, say, *i.e.*

$$\sigma(r) = \left(\frac{\sigma_0}{r_0}\right) \sqrt{r^2 + r_0^2},$$

and cover the retina with such $\sigma(r)$ -discs, we can count the number of such discs in the foveal region $0 \leq r < \rho$, and in the periphery $\rho \leq r < R$. For simplicity we model the fovea as a flat disc of radius R . The fractional covering of $\sigma(r)$ -discs inside a ring of width dr at eccentricity r equals $2\pi r dr$ divided by $\pi\sigma^2(r)$, the area of such a disc. Therefore, the respective numbers in the foveal and peripheral regions are

$$\begin{aligned} \mathcal{N}_f &= \left(\frac{r_0}{\sigma_0}\right)^2 \int_0^\rho \frac{2r dr}{r^2 + r_0^2} = \left(\frac{r_0}{\sigma_0}\right)^2 \ln \frac{\rho^2 + r_0^2}{r_0^2}, \\ \mathcal{N}_p &= \left(\frac{r_0}{\sigma_0}\right)^2 \int_\rho^R \frac{2r dr}{r^2 + r_0^2} = \left(\frac{r_0}{\sigma_0}\right)^2 \ln \frac{R^2 + r_0^2}{\rho^2 + r_0^2}. \end{aligned}$$

If we now define ρ through the equation

$$\mathcal{N}_f = \mathcal{N}_p,$$

we obtain

$$\left(\frac{\rho}{r_0}\right)^2 + 1 = \sqrt{\left(\frac{R}{r_0}\right)^2 + 1},$$

which is independent of σ_0 , but does depend on the choice of r_0 , or rather the ratio $\epsilon = r_0/R$:

$$\frac{\rho}{R} = \epsilon^{\frac{1}{2}} \left((1 + \epsilon^2)^{\frac{1}{2}} - \epsilon \right)^{\frac{1}{2}} = \epsilon^{\frac{1}{2}} + \mathcal{O}(\epsilon^{\frac{3}{2}}). \quad (17)$$

Let us define the retinotopic cortical magnification m as the ratio of the foveal area $\mathcal{A}_f = \pi \rho^2$ to the full retinal area $\mathcal{A}_r = \pi R^2$:

$$m = \frac{\mathcal{A}_f}{\mathcal{A}_r} = \left(\frac{\rho}{R}\right)^2 \approx \epsilon,$$

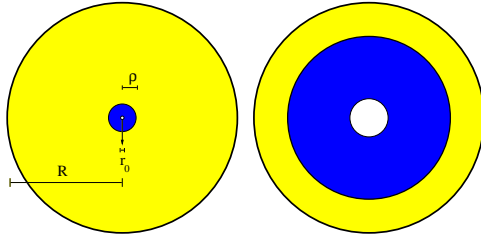


Figure 4: Left: Decomposition of the retina into three nested regions: R is the radius of the entire retina, ρ is the radius demarcating a foveal neighbourhood containing 50% of the receptive field loci, whereas r_0 is the radius of the fovea. Relative estimates are given in the text. Right: Same regions after cortical magnification.

where the latter approximation holds if $\varepsilon \ll 1$ so that we may ignore the higher order terms in Eq. (17). In the case of human vision it is estimated that about half of the human striate cortex is devoted to a foveal region covering roughly 1–2% of the visual field [38]. Thus in this case $\varepsilon \approx 0.015 \pm 0.005$, from which we deduce that the constant in the conformal metric, Eq. (14), equals $r_0 \approx (0.015 \pm 0.005) R$, which is roughly the correct radius of the human fovea. Moreover, $\rho \approx (0.12 \pm 0.02) R$, again not an unrealistic estimate. To get a feeling for all these scales, *cf.* Fig. 4.

Note that Eq. (15) and Eq. (16) are alternative interpretations of the retinal scaling law: Log-polar transform and eccentricity scaling are close-knit. Unlike the latter, however, the former does not explain the resolution limitation of the fovea.

3 Conclusion and Discussion

Retinocortical mechanisms can be understood in terms of a fibre bundle construct over a Riemannian manifold endowed with a conformal metric. The metric can be constructed in an axiomatic fashion up to a pair of parameters, which can be matched to empirics. Phenomenological facts such as the Weber-Fechner law, the retinotopical cortical magnification, and the way in which typical receptive field size scales with eccentricity can be incorporated in a fairly straightforward manner. There is quantitative agreement with a couple of known facts on human retinocortical mechanisms.

The advantage of a geometric model over any *ad hoc* model is that it brings in only necessary parameters with geometric significance. Moreover, the axiomatic underpinning enables a systematic refinement of the model, which facilitates generalisation to account for other known phenomena and also increases its predictive potential.

A suggestion for future work may be to account for some form of (affine) connection and its relation to known neural substrates (horizontal cells?). The inclusion of temporal mechanisms should pose no problems in principle [2, 1, 18]. Subsequently one should turn to the exploration of spatiotemporal aspects in general, such as motion selectivity (amacrine cells?), Reichardt detectors [37], and “separable/inseparable” spatiotemporal receptive fields in general [4, 6]. Finally, the many feedback loops that are known to exist at the retinal stage as well as between LGN and V1 may have geometric significance as well (selecting sections through the fibre bundle?).

References

- [1] D. A. Baylor. Photoreceptor signals and vision. *Investigative Ophthalmology and Visual Science*, 28:34–49, January 1987. Proctor Lecture.
- [2] D. A. Baylor, B. J. Nunn, and J. L. Schnapf. The photocurrent, noise and spectral sensitivity of rods of the monkey *Macaca fascicularis*. *Journal of Physiology*, 357:575–607, 1984.
- [3] P. Bijl. *Aspects of Visual Contrast Detection*. PhD thesis, University of Utrecht, Department of Physics, Utrecht, The Netherlands, May 8 1991.
- [4] D. Cai, G. C. DeAngelis, and R. D. Freeman. Spatiotemporal receptive field organization in the lateral geniculate nucleus of cats and kittens. *Journal of Neurophysiology*, 78(2):1045–1061, August 1997.
- [5] Y. Choquet-Bruhat, C. DeWitt-Morette, and M. Dillard-Bleick. *Analysis, Manifolds, and Physics. Part I: Basics*. Elsevier Science Publishers B.V. (North-Holland), Amsterdam, 1991.
- [6] G. C. DeAngelis, I. Ohzawa, and R. D. Freeman. Receptive field dynamics in the central visual pathways. *Trends in Neuroscience*, 18(10):451–458, 1995.
- [7] B. Fischer and H. U. May. Invarianzen in der Katzenretina: Gesetzmäßige Beziehungen zwischen Empfindlichkeit, Größe und Lage rezeptiver Felder von Ganglienzellen. *Experimental Brain Research*, 11:448–464, 1970.
- [8] L. M. J. Florack. *Image Structure*, volume 10 of *Computational Imaging and Vision Series*. Kluwer Academic Publishers, Dordrecht, The Netherlands, 1997.
- [9] L. M. J. Florack. Non-linear scale-spaces isomorphic to the linear case. In B. K. Ersbøll and P. Johansen, editors, *Proceedings of the 11th Scandinavian Conference on Image Analysis (Kangerlussuaq, Greenland, June 7–11 1999)*, volume 1, pages 229–234, Lyngby, Denmark, 1999.
- [10] L. M. J. Florack, R. Maas, and W. J. Niessen. Pseudo-linear scale-space theory. *International Journal of Computer Vision*, 31(2/3):247–259, April 1999.
- [11] L. M. J. Florack, A. H. Salden, B. M. ter Haar Romeny, J. J. Koenderink, and M. A. Viergever. Nonlinear scale-space. In B. M. ter Haar Romeny, editor, *Geometry-Driven Diffusion in Computer Vision*, volume 1 of *Computational Imaging and Vision Series*, pages 339–370. Kluwer Academic Publishers, Dordrecht, 1994.
- [12] B. M. ter Haar Romeny, L. M. J. Florack, J. J. Koenderink, and M. A. Viergever, editors. *Scale-Space Theory in Computer Vision: Proceedings of the First International Conference, Scale-Space’97, Utrecht, The Netherlands*, volume 1252 of *Lecture Notes in Computer Science*. Springer-Verlag, Berlin, July 1997.
- [13] J. J. Koenderink. The concept of local sign. In A. J. van Doorn, W. A. P. F. L. van de Grind, and J. J. Koenderink, editors, *Limits in Perception*, pages 495–547. VNU Science Press, Utrecht, 1984.
- [14] J. J. Koenderink. The structure of images. *Biological Cybernetics*, 50:363–370, 1984.

- [15] J. J. Koenderink. The structure of the visual field. In W. Güttlinger and G. Dangelmayr, editors, *The Physics of Structure Formation: Theory and Simulation. Proceedings of an International Symposium*, Tübingen, Germany, October 27–November 2 1986. Springer-Verlag.
- [16] J. J. Koenderink. Design for a sensorium. In W. von Seelen, G. Shaw, and U. M. Leinhos, editors, *Organization of Neural Networks - Structures and Models*, pages 185–207. VCH Verlagsgesellschaft mbH, Weinheim, Germany, 1988.
- [17] J. J. Koenderink. Design principles for a front-end visual system. In R. Eckmiller and Ch. v. d. Malsburg, editors, *Neural Computers*, volume 41 of *NATO ASI Series F: Computer and Systems Sciences*, pages 111–118. Springer-Verlag, Berlin, 1988.
- [18] J. J. Koenderink. Scale-time. *Biological Cybernetics*, 58:159–162, 1988.
- [19] J. J. Koenderink. A hitherto unnoticed singularity of scale-space. *IEEE Transactions on Pattern Analysis and Machine Intelligence*, 11(11):1222–1224, November 1989.
- [20] J. J. Koenderink. The brain a geometry engine. *Psychological Research*, 52:122–127, 1990.
- [21] J. J. Koenderink. Mapping formal structures on networks. In T. Kohonen, K. Mäkisara, O. Simula, and J. Kangas, editors, *Artificial Neural Networks*, pages 93–98. Elsevier Science Publishers B.V. (North-Holland), 1991.
- [22] J. J. Koenderink. Local image structure. In P. Johansen and S. Olsen, editors, *Theory & Applications of Image Analysis*, volume 2 of *Series in Machine Perception and Artificial Intelligence*, pages 15–21. World Scientific, Singapore, 1992. Selected papers from the 7th Scandinavian Conference on Image Analysis.
- [23] J. J. Koenderink. What is a “feature”? *Journal of Intelligent Systems*, 3(1):49–82, 1993.
- [24] J. J. Koenderink and A. J. van Doorn. Dynamic shape. *Biological Cybernetics*, 53:383–396, 1986.
- [25] J. J. Koenderink and A. J. van Doorn. Logical stratification of organic intelligence. In R. Trappl, editor, *Cybernetics and Systems*, pages 871–878. D. Reidel Publishing Company, 1986.
- [26] J. J. Koenderink and A. J. van Doorn. Representation of local geometry in the visual system. *Biological Cybernetics*, 55:367–375, 1987.
- [27] J. J. Koenderink and A. J. van Doorn. The basic geometry of a vision system. In R. Trappl, editor, *Cybernetics and Systems*, pages 481–485. Kluwer Academic Publishers, 1988.
- [28] J. J. Koenderink and A. J. van Doorn. The structure of locally orderless images. *International Journal of Computer Vision*, 31(2/3):159–168, April 1999.
- [29] J. J. Koenderink, A. Kappers, and A. J. van Doorn. Local operations: The embodiment of geometry. In G. A. Orban and H.-H. Nagel, editors, *Artificial and Biological Vision Systems*, Basic Research Series, pages 1–23. Springer Verlag, Berlin, 1992.
- [30] J. J. Koenderink and A. J. van Doorn. Operational significance of receptive field assemblies. *Biological Cybernetics*, 58:163–171, 1988.

- [31] J. J. Koenderink and A. J. van Doorn. Receptive field families. *Biological Cybernetics*, 63:291–298, 1990.
- [32] J. J. Koenderink and A. J. van Doorn. Receptive field taxonomy. In R. Eckmiller, editor, *Advanced Neural Computers*, pages 295–301. Elsevier Science Publishers B.V. (North-Holland), 1990.
- [33] J. J. Koenderink and A. J. van Doorn. Receptive field assembly pattern specificity. *Journal of Visual Communication and Image Representation*, 3(1):1–12, 1992.
- [34] J. J. Koenderink and A. J. van Doorn. Local image operators and iconic structure. In G. Sommer and J. J. Koenderink, editors, *Algebraic Frames for the Perception-Action Cycle: Proceedings of the International Workshop, AFPAC'97 (Kiel, Germany, September 1997)*, volume 1315 of *Lecture Notes in Computer Science*, pages 66–93, Berlin, September 1997. Springer-Verlag.
- [35] T. Lindeberg. *Scale-Space Theory in Computer Vision*. The Kluwer International Series in Engineering and Computer Science. Kluwer Academic Publishers, Dordrecht, The Netherlands, 1994.
- [36] P. J. Olver. *Applications of Lie Groups to Differential Equations*, volume 107 of *Graduate Texts in Mathematics*. Springer-Verlag, 1986.
- [37] W. Reichardt. Autocorrelation, a principle for the evaluation of sensory information by the central nervous system. In W. A. Rosenblith, editor, *Sensory Communication*, pages 303–317. MIT Press, Cambridge, 1961.
- [38] R. W. Rodieck. *The First Steps in Seeing*. Sinauer Associates, Inc., Sunderland, Massachusetts, 1998.
- [39] L. Schwartz. *Théorie des Distributions*, volume I, II of *Actualités scientifiques et industrielles; 1091,1122*. Publications de l'Institut de Mathématique de l'Université de Strasbourg, Paris, 1950–1951.
- [40] M. Spivak. *Differential Geometry*, volume 1–5. Publish or Perish, Berkeley, 1975.
- [41] J. Sporring, M. Nielsen, L. M. J. Florack, and P. Johansen, editors. *Gaussian Scale-Space Theory*, volume 8 of *Computational Imaging and Vision Series*. Kluwer Academic Publishers, Dordrecht, The Netherlands, 1997.
- [42] F. W. Weymouth. Visual sensory units and the minimal angle of resolution. *American Journal of Ophthalmology*, 46:102–113, 1958.
- [43] A. P. Witkin. Scale-space filtering. In *Proceedings of the International Joint Conference on Artificial Intelligence*, pages 1019–1022, Karlsruhe, Germany, 1983.
- [44] R. A. Young. The Gaussian derivative model for machine vision: Visual cortex simulation. *Journal of the Optical Society of America*, July 1986.
- [45] R. A. Young. The Gaussian derivative model for machine vision: I. retinal mechanisms. *Spatial Vision*, 2(4):273–293, 1987.